Chapter 5

β-Cyclodextrin-polyurethane magnetic nanoconjugates for targeted drug delivery in cancer therapy

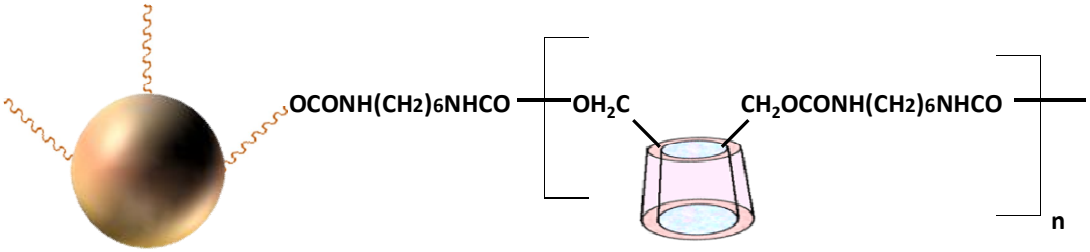

CYD-PU-NPs

III

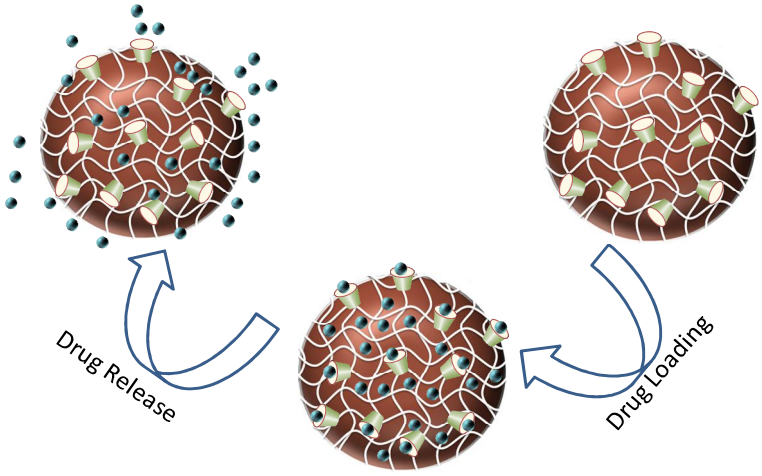

Subsequent to the synthesis of pH responsive PUs, our focus was to develop nanosized carriers for targeted drug delivery. The magnetic nanoparticles such as iron oxide have found broad range of applications in the field of medicine and biology such as controlled drug delivery, protein purification, specific cell targeting and medical imaging [1–3]. This is due to their exceptional combination of properties including adaptability for external manipulation [4], controlled size and enhancement of contrast in magnetic resonance imaging (MRI) [5]. On the other hand, Cyclodextrins are one of the most versatile systems in pharmaceutical applications for their unique structural design [6]. They have ability to form inclusion complexes with a wide range of drugs and macromolecules thereby altering their physical, chemical and biological properties [7–12]. A system with combination of Cyclodextrin and magnetic nanoparticles can give synergistic advantage of both enhanced bioavailability of drug and magnet responsive transport respectively. Hence, we explored a strategy to conjugate MNPs (magnetic nanoparticles) covalently with β-Cyclodextrin-PUs to prepare magnetic PU nanocarriers for anti-cancer drugs.

5.1. INTRODUCTION

The magnetic characteristic of Fe_3O_4 nanoparticles is beneficial in two ways. First, the particles can respond to external magnetic field for easy magnetic guided transport field [1,2] and second; the aggregation of particles can be avoided since they possess no magnetization after removal of magnetic field [3] and can be tracked by MRI [5]. The mandatory requirement for the MNPs to be adopted in biomedical and bioengineering field is that they shall possess high magnetization values along with the nano size (<100nm). They shall also possess narrow particle size distribution in order to facilitate uniformity in the properties [13]. Besides this, such applications

also need the coating of the MNPs with biocompatible materials that can act as a base for targeted drug delivery applications. The coating/covalent bonding of MNPs with polymeric materials also aids to get rid of the agglomeration of MNPs [14], which is a most annoying problem generally faced while handling the MNPs.

Cyclodextrins are known to possess toroidal shape with hydrophilic exterior and lipophilic interior cavity. Due to this, they have ability to form inclusion complexes with a wide range of drugs and macromolecules thereby altering their physical, chemical and biological properties (Fig. 5.1 (a)).

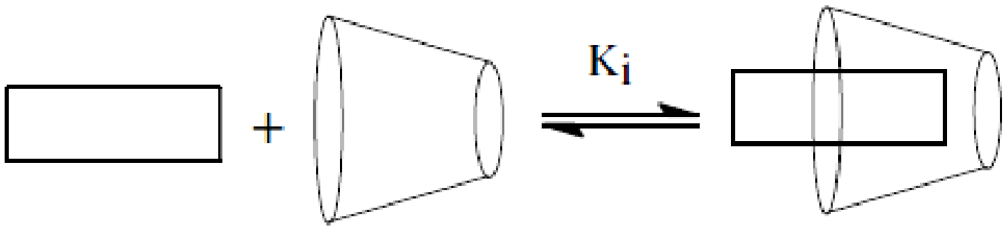

Figure 5.1(a) Illustration of formation of host-guest complex according to an equilibrium process where Ki is the 1:1 equilibrium binding constant, toroid represent β-Cyclodextrin, rectangle represent guest molecule.*(Reproduced from Mohammad et al*) [15].

This aids in achieving enhanced bioavailability, solubility and stability of drug molecules. There are numerous factors that makes cyclodextrins best suitable as drug carriers; like availability of potential sites for modification, low pharmacological activity, protection of included drug molecules from biodegradation, low toxicity etc.[16]. Chemically, Cyclodextrins possess cyclic structure consisting of six, seven or eight α-D-glucopyranose units connected by α-(1→4) linkages commonly referred to as α-, β-, and γ-CDs, respectively [7].

β-Cyclodextrin (Fig. 5.1(b)) contains 21 hydroxyl groups (7 primary and 14 secondary) which can be utilized for its further conjugation and structural modification to obtain its derivatives by tuning the stoichiometry. The very popular characteristics of its dual polarity is due to non polar interior owned by presence of glycosidic oxygens & methine protons and polar exterior by the virtue of presence of hydroxyl groups [17]. The polymerized Cyclodextrin is superior over parent cyclodextin for application in the drug delivery field in the sense that it combines the advantage of the versatile properties of polymer and parent Cyclodextrin [18].

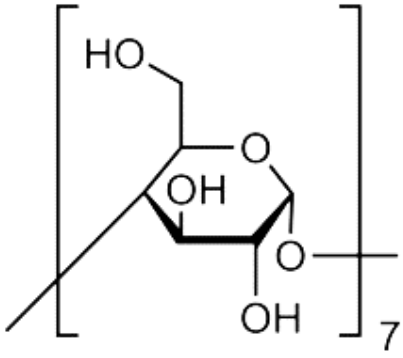

Figure 5.1(b) Structure of β-Cyclodextrin

A system with combination of Cyclodextrin and magnetic nanoparticles can give synergistic advantage of both enhanced bioavailability of drug and magnet responsive transport respectively. The design of such system was possible due to presence of hydroxyl groups on both the moieties, which can be linked to isocyanate molecules to form polyurethane (PU) polymer. The added advantage of polyurethane polymer is its biocompatibility, stability, strength and adaptability for modification which enhances applicability[19]. Copolymers of Cyclodextrin have been reported to form host-guest complexes comparable to native Cyclodextrins. The copolymer of epichlorohydrin with β-Cyclodextrin has been recently explored for its intended application in drug

delivery system [20] and electrochemical probe in aqueous solution [21]. Similarly hydroxypropyl Cyclodextrin [22], PU based on β-CD [23] and randomly methylated Cyclodextrin have been reported for inclusion complex formation [24]. The structure of copolymer can be systematically varied in order to tune the inclusion sites of cyclodextin [15]. As shown in Fig. 5.1(c), the variation in the molar content of isocyanate leads to variation of surface accessible inclusion sites of Cyclodextrin.

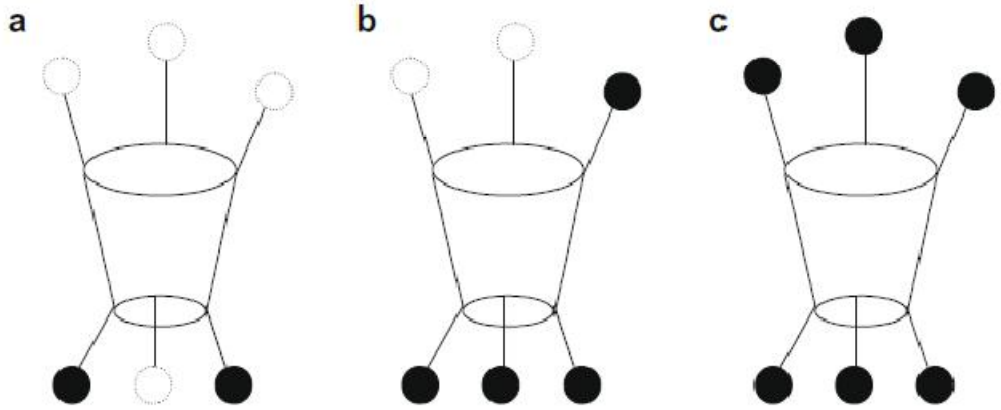

Figure 5.1(c) Schematic diagram showing the substitution of primary (narrow end) and secondary (wide end) hydroxyl groups by isocyanate crosslinker in the annular regions of a β-CD copolymer: (a) β -CD:linker (1:1), and (b) β -CD:linker (1:2), and (c) β -CD:linker (1:3) reactant ratios. The solid spheres represent covalently attached sites and open spheres represent available (unreacted) sites.*(Reproduced from Mohammad et al)* [15]

Specifically, in case of PUs, this task is more feasible as it can be achieved by variation of mole ratio of NCO/OH [25,26]. The Cyclodextrin based PUs have been reported by reaction of Cyclodextrin with isocyanate for the intended applications like adsorbents, binder for active pharmaceutical ingredients and molecular imprinting [27], however its application as a controlled drug delivery system has been largely unexplored. There is dual advantage since both Cyclodextrin cavity as well as PU network can encapsulate drug. Hence, we expected high drug payload. We explored a

strategy to conjugate MNPs covalently with β-Cyclodextrin-PUs to prepare magnetic PU nanocarriers for anti-cancer drugs. For comparison, the conjugates were also prepared with PEG instead of β-Cyclodextrin. In order to define effect of variation of accessible sites of Cyclodextrin on drug release, nanoconjugates were synthesized with different mole ratios.

Dacarbazine (DCR), 5-(3,3-dimethyl-1-triazeno)-imidazole-4-carboxamide (Fig. 5.2) is prodrug frequently used as cancer chemo therapeutic agent, particularly for the treatment of malignant melanoma [28]. In cases of advanced stages of cancer the dacarbazine has been used in combination with other drugs for treatment of malignant melanoma, Hodgkin's lymphoma, soft-tissue sarcomas, and childhood solid tumors [29]. The mechanism of action involves alkylation of nucleic acids through methylation leading to covalent linkages with sulfhydryl groups. This in turn inhibits DNA replication resulting in cell death [30]. The main disadvantage of chemotherapy is that more than half of the available chemotherapeutic drugs show serious side effects developed in the patient's body due to lack of tumor specific uptake and bioavailability resulting in the damage of healthy tissues [31]. The discomfort associated with such side effects is more painful than the disease itself. One of the strategies to avoid this trauma is application of magnetic drug targeting [28]. Also, the nano emulsion of dacarbazine is reported to be more effective towards cancer therapy in xenograft mouse epidermoid carcinoma model as compare to dacarbazine suspension [32]. Hence, we have attempted to investigate magnetic drug targeting by employing PU conjugated magnetic nanocarriers using Dacarbazine as a model drug.

5.2. MATERIALS AND METHODS

5.2.1 MATERIALS

β-Cyclodextrin, polyethylene glycol (PEG 6000), Fe_3O_4 nanoparticles and hexamethylene diisocyanate (HMDI) were purchased from Sigma Aldrich, India. Dimethyl formamide (DMF) was purchased from Qualigens, Bombay, India. Dacarbazine was purchased from Sigma Aldrich, India and used as received. Phosphate buffer saline tablets (for preparation of pH 7.4 buffer solution) were obtained from Sigma Aldrich, India.

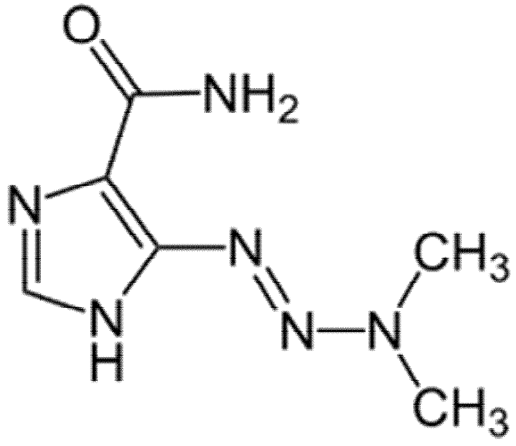

Figure 5.2 Structure of Dacarbazine

5.2.2 SYNTHESIS OF PU-MNP NANOCONJUGATES

The synthesis of PU-MNP nanoconjugates is illustrated in Scheme 1. Fe_3O_4 nanoparticles (0.4 g) were dispersed in DMF (60 mL) by sonication. HMDI (1.767g in 10 mL DMF) was added drop wise during the course of 15 min [33]. The reaction mixture was sonicated for next 3h. β-Cyclodextrin (2g, dissolved in 30 mL DMF) was then added drop wise. The reaction was allowed to proceed at 70°C for next 3h. The product was separated by magnetic decantation followed by washings of acetone and water. The CYD-PU-NPs were dried in vacuum for 24h. Using Similar procedure, we

have synthesized three nanocarriers with the mole ratio of Cyclodextrin:HMDI of 1:1, 1:2 and 1:3 namely CYD-PU-11, CYD-PU-12, and CYD-PU-13 respectively. Similar procedure was adopted for synthesis of PEG-PU-NPs with PEG:HMDI mole ratio 1:2. Copolymer of HMDI and Cyclodextrin with Cyclodextrin:HMDI mole ratio 1:2 and Copolymer of HMDI and PEG with PEG:HMDI mole ratio 1:2 were prepared by same method as described above, in order to carry out DSC analysis.

5.2.3 CHARACTERIZATION

The FTIR spectra were recorded as KBr discs on a PerkinElmer IR spectrophotometer at room temperature. Thermo gravimetric analysis (TGA) was carried out by using TG–DTA 6300 INCARP EXSTAR 6000 in the temperature range of 30–600°C and heating rate of 10°C/min. The nitrogen atmosphere was maintained throughout the measurement. Differential scanning calorimetry (DSC) thermograms were recorded on a NETZSCH DSC at a rate of 10°C /min under nitrogen with 30–40 mL/min gas flow rate and temperature range of -100 to 200°C. The DSC analysis was carried out under both cooling and heating cycles. Vibrating sample magnetometer (VSM) analysis was carried out by using Lakeshore VSM 7410 at room temperature. Jeol (Jem-2100) electron microscope was used at an acceleration voltage of 200 kV in order to carry out High-Resolution Transmission Electron Microscopy (HR-TEM) analysis. Energy dispersive X-ray (EDX) analysis of the vacuum dried CYD-PU-NPs was recorded by the model-JSM-5610 LV attached to Scanning electron microscopy (SEM). X-ray diffraction (XRD) was carried out by using PANalytical 'X'PERT-PRO XRPD of Cu Kα radiation (λ= 0.15406 nm) with a scanning rate of 2°/min and 2θ ranging from 0 to 100°.

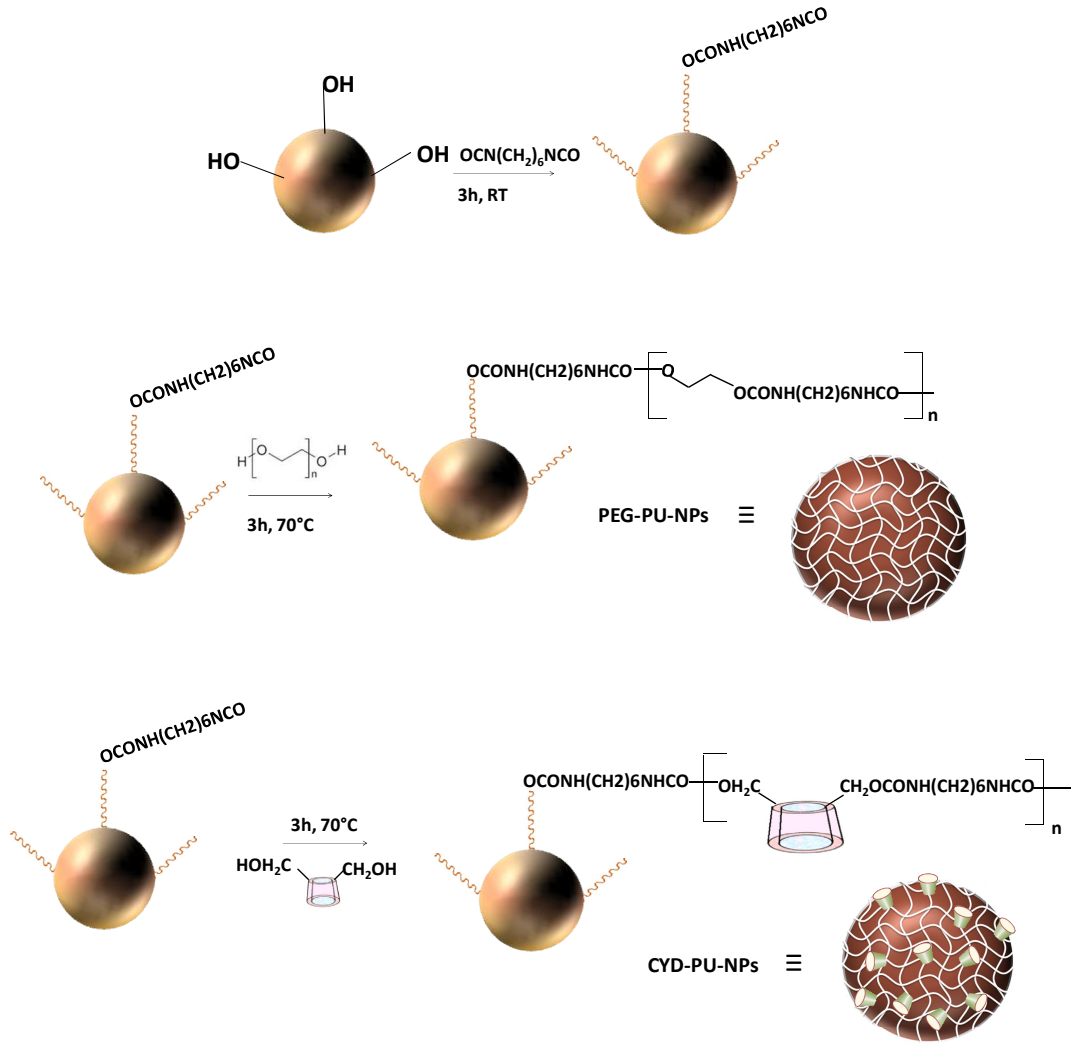

Scheme 5.1 Synthesis of PU-MNP nanoconjugates

5.2.4 Preparation of Dacarbazine loaded PU-MNP nanoconjugates

The loading of Dacarbazine on PU-MNP nanoconjugates was investigated through batch technique [34]. The Dacarbazine solution (30mg/mL) was prepared by dissolving 150mg Dacarbazine in 5mL ethanol followed by addition of 45mL water. For loading of drug on the nanoparticles, 15mg of nanoparticles were suspended in a vial containing 5mL of 30mg/mL Dacarbazine solution. The mixture thus obtained was sonicated overnight at room temperature under dark conditions. The drug-loaded nanoparticles were separated from the free drug by magnetic decantation and washed

twice with ethanol. The drug-loaded nanoparticles were allowed to dry at room temperature for 24h and then stored in desiccators. The concentration of drug in supernatant was determined by using calibration plot constructed on UV-Spectrophotometer for Dacarbazine at 360nm. The drug entrapment efficiency (%LE) of CYD-PU-NPs was estimated by using following equation [35].

$$\%\ enrapment\ efficiency = \frac{Ic-Sc}{Ic} \times 100 \quad \text{---------- (1)}$$

Where I_C denotes initial content of Dacarbazine added and S_C represents Dacarbazine concentration in supernatant. Care was taken to maintain dark conditions throughout drug loading and release studies as Dacarbazine is reported to degrade in light [36].

5.2.5 Swelling studies of PU MNP nanoconjugates

In order to study the swelling properties of PU MNP nanoconjugates, the known weight of PEG-PU-NPs and CYD-PU-NPs were kept in phosphate buffer saline (0.1 M, pH 7) at 37°C for 24h. The swelling of polymers was measured by equilibrium weight gain method [37]. Following equation was used to carry out calculations for determination of equilibrium swelling (Q), where W_1 and W_2 denote the weight of polymer before and after equilibrium swelling respectively. The swelling experiments were performed in triplicate and the mean value of Q was tabulated.

$$Q = \left(\frac{W_2 - W_1}{W_1}\right) \times 100 \quad \text{---------- (2)}$$

5.2.6 Cell culture and measurement of cell viability by MTT assay

The normal lung cell line L132 was obtained from National Centre for Cell Sciences, Pune, India. Cell viability was evaluated by MTT (3-[4,5-dimethylthiazol-2-yl]-

2,5diphenyltetrazolium bromide, Sigma–Aldrich) biochemical assay as per a reported procedure [38]. Three replicates were performed for each set of nanoparticles and the mean values are reported.

5.3. RESULTS AND DISCUSSION

5.3.1 SYNTHESIS OF PU-MNP NANOCONJUGATES

Fe_3O_4 nanoparticles are characterized with presence of free hydroxyl groups on its surface [39,40] which makes them prone to react with isocyanate. When MNPs are allowed to react with excess of isocyanate, NCO functionalized MNPs result. The free NCO end groups can further react with β-Cyclodextrin/PEG. As described above, β-Cyclodextrin is having 7 primary hydroxyl groups per molecule, which is advantageous to precede reaction with isocyanate groups. The interesting part is that, by varying the isocyanate in-situ, one can have command over reaction between numbers of hydroxyl groups of β-Cyclodextrin that can react with isocyanate. Increasing β-Cyclodextrin:isocyanate mole ratio leads to increased isocyanate content, which results into utilization of higher number of hydroxyl groups of β-Cyclodextrin leading to formation of PU with higher crosslink density. As per Mohamed et al, as the mole ratio of β-Cyclodextrin:isocyanate increases from 1:1 to 1:3, the NCO group of isocyanate also gets covalently attached to the secondary hydroxyl groups of β-Cyclodextrin, resulting into lesser number of accessible inclusion sites [15]. Since the number of hydroxyl groups determines the cavity size [41], we have hypothesized that the size of cavity reduces with increase in β-Cyclodextrin:isocyanate.

5.3.2 IR SPECTROSCOPY

The structure of nanoconjugates was confirmed by characteristic peaks obtained in IR spectra. As shown in Fig. 5.3, the FT-IR spectrum of β-Cyclodextrin was

characterized by a single broad band at 3300–3500 cm^{-1} corresponding to O-H stretching vibrations. Vibrations of the C-H and CH_2 groups appeared in the 2800–3000 cm^{-1} region. IR of CYD-PU-NPs showed peaks at 553 cm^{-1}, 1623 cm^{-1}, and 3316 cm^{-1}, corresponding to Fe-O bonds in tetrahedral sites for Fe-nanoparticles, N-H and C=O bond for PU respectively [33].

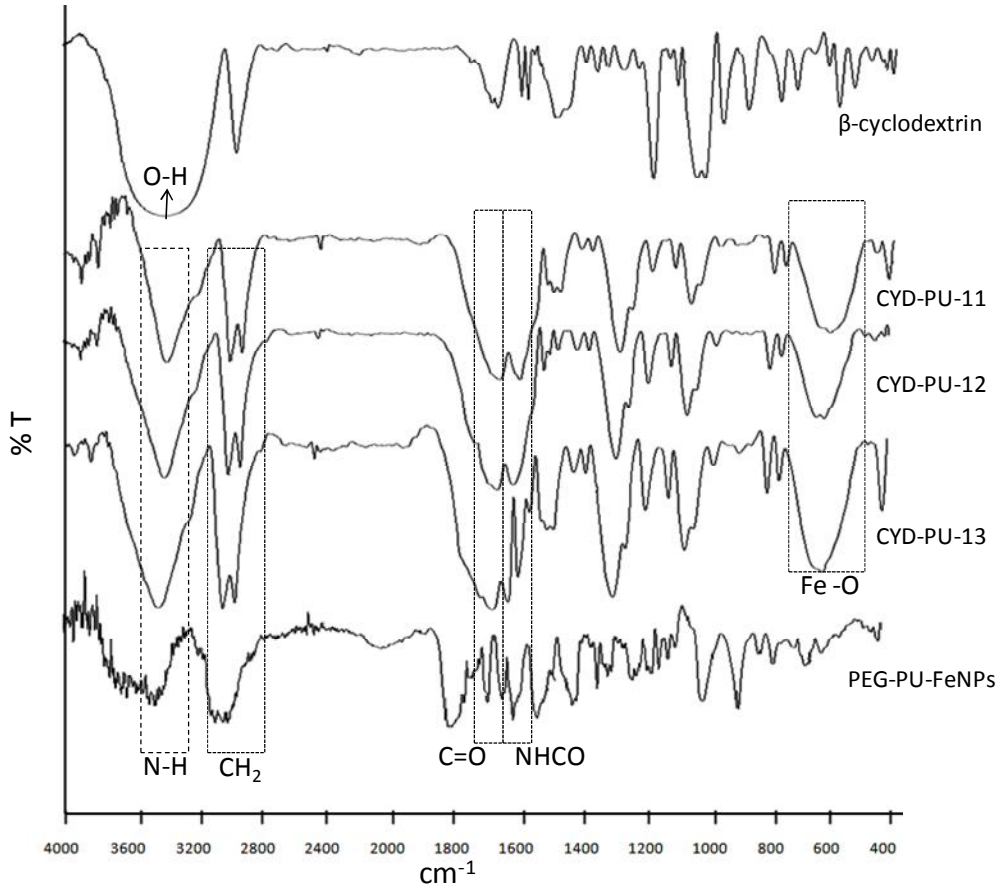

Figure 5.3 FTIR spectra of β-Cyclodextrin and PU-MNP nanoconjugates

The NHCO stretching was also observed at 1560 cm^{-1}.The absorption bands at 2852 and 2863 cm^{-1} were attributed to -CH_2-stretching vibrations. Similarly, structure of PEG-PU-NPs was verified by peaks obtained at 580 cm^{-1}, 1743 cm^{-1} and 3312 cm^{-1} corresponding to Fe-O bonds in tetrahedral sites for Fe-nanoparticles, N-H and C=O

bond for PU respectively. Peaks obtained at 1576 cm^{-1} and 2863 cm^{-1} were assigned to NHCO stretching and -CH_2- stretching vibrations.

5.3.3 THERMAL ANALYSIS

The nanoconjugates were analyzed for thermal properties using TGA and DSC. As shown in Fig 5.4(a), the TGA plots of CYD-PU-NPs suggests that it exhibits three-stage degradation pattern over the range of 30-600°C, which is in accordance with the previous report [33]. The first stage of weight loss below approximately 200°C can be attributed to the loss of surface adsorbed water as well as dehydration of surface OH groups. The second stage of weight loss of around 10-50% was observed between temperature range of 276 to 344°C, which can be due to cleavage of urethane linkage. This temperature range for urethane bond degradation is quite high as compared to other conventional polyurethanes with carbohydrate crosslinkers like glucose, starch, cellulose that generally start degrading at temperatures as low as 200°C [26,42]. The last stage of degradation in the region of 344–470°C, probably, is due to thermal decomposition of Cyclodextrin [33]. It is apparent from the TGA data that the PEG-PU-NPs were observed to be thermally more stable. PEG is high molecular weight polyol, which apart from forming urethane linkage also coats the surface of MNPs. This results in enhancement of thermal properties. Amongst CYD-PNPs, it was observed that the degradation follows entirely different pattern during initial and later degradation stages. Before 5wt% degradation, the degradation temperature is observed to be highest for CYD-PU-11 (Table 5.1), and decreases with increasing β-Cyclodextrin:HMDI mole ratio. As the initial degradation is attributed to loss of both the surface adsorbed water and dehydration of surface OH groups, content of both surface adsorbed water and surface OH groups shall be in the order CYD-PU-11> CYD-PU-12> CYD-PU-13. The higher content of surface OH groups in case of

CYD-PU-11 as compared to CYD-PU-12 and CYD-PU-13 is apparent since increasing β-Cyclodextrin:HMDI mole ratio leads to increased utilization of hydroxyl groups of β-Cyclodextrin due to higher content of isocyanate groups. The second stage of degradation beyond 5wt% follows exactly opposite trend i.e. degradation temperature is in the order of CYD-PU-11< CYD-PU-12< CYD-PU-13. The second stage of degradation is attributed to degradation of urethane linkage. The degree of crosslinking increases as we move from CYD-PU-11 to CYD-PU-12 to CYD-PU-13 due to increase in β-Cyclodextrin:HMDI mole ratio. Since the highly crosslinked PUs are characterized with high degradation temperatures [43], the results obtained here are obvious.

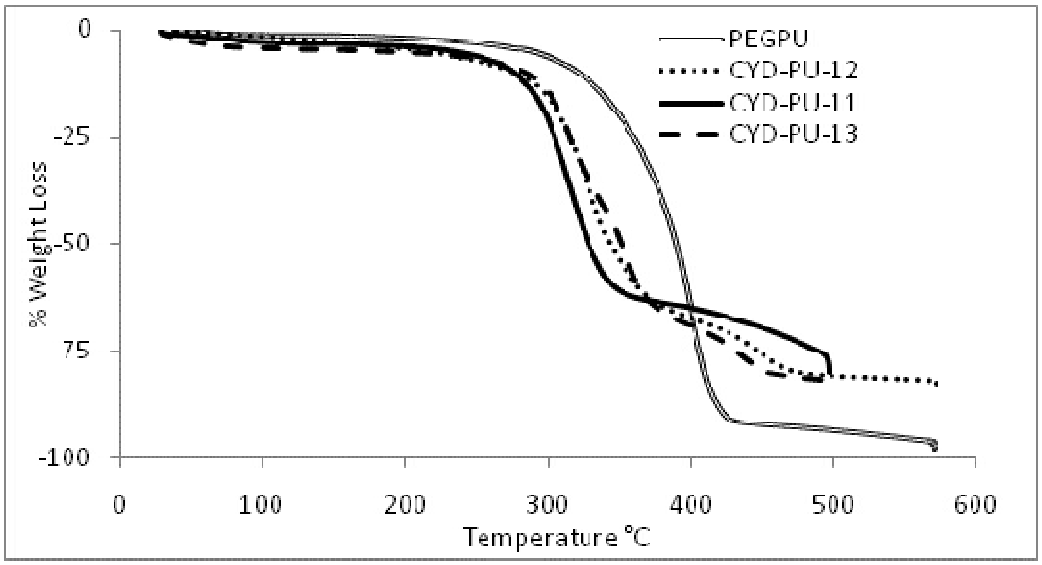

Figure 5.4 (a) Thermal degradation plots of PU-MNP nanoconjugates

DSC thermograms for both heating [Fig 5.4b(A)] and cooling [Fig 5.4b(B)] cycles of the synthesized PUs are shown in Fig 5.4b. The PUs are characterized with phase segregation due to presence of dual phases namely soft and hard segments [44]. Due to this special characteristic, the PUs may show two distinct glass transition

temperatures corresponding to hard and soft segment namely T_{gHS} and T_{gSS} respectively [45]. In addition, the glass transition temperature of PUs depends strongly on the molecular mobility and the PUs with higher crosslinked structure are characterized with higher values of glass transition temperatures [45].

Table 5.1 Thermal degradation temperature of PU-MNP nanoconjugates

Wt Loss (%)	**Degradation Temperature° C**			
	CYD-PU-11	CYD-PU-12	CYD-PU-13	PEG-PU-NPs
1	033.26	032.89	030.95	073.15
2	063.87	050.28	041.24	204.84
5	230.98	222.71	186.22	288.72
10	275.98	289.22	284.78	321.66
50	328.85	349.92	350.91	390.21
80	496.69	497.35	453.05	410.12

Table 5.2 Glass transition temperature of copolymers

Polymer	**T_{gSS}**	**T_{gHS}**
CYD-PU	-11.6	81
PEG-PU	-32.8	67.2

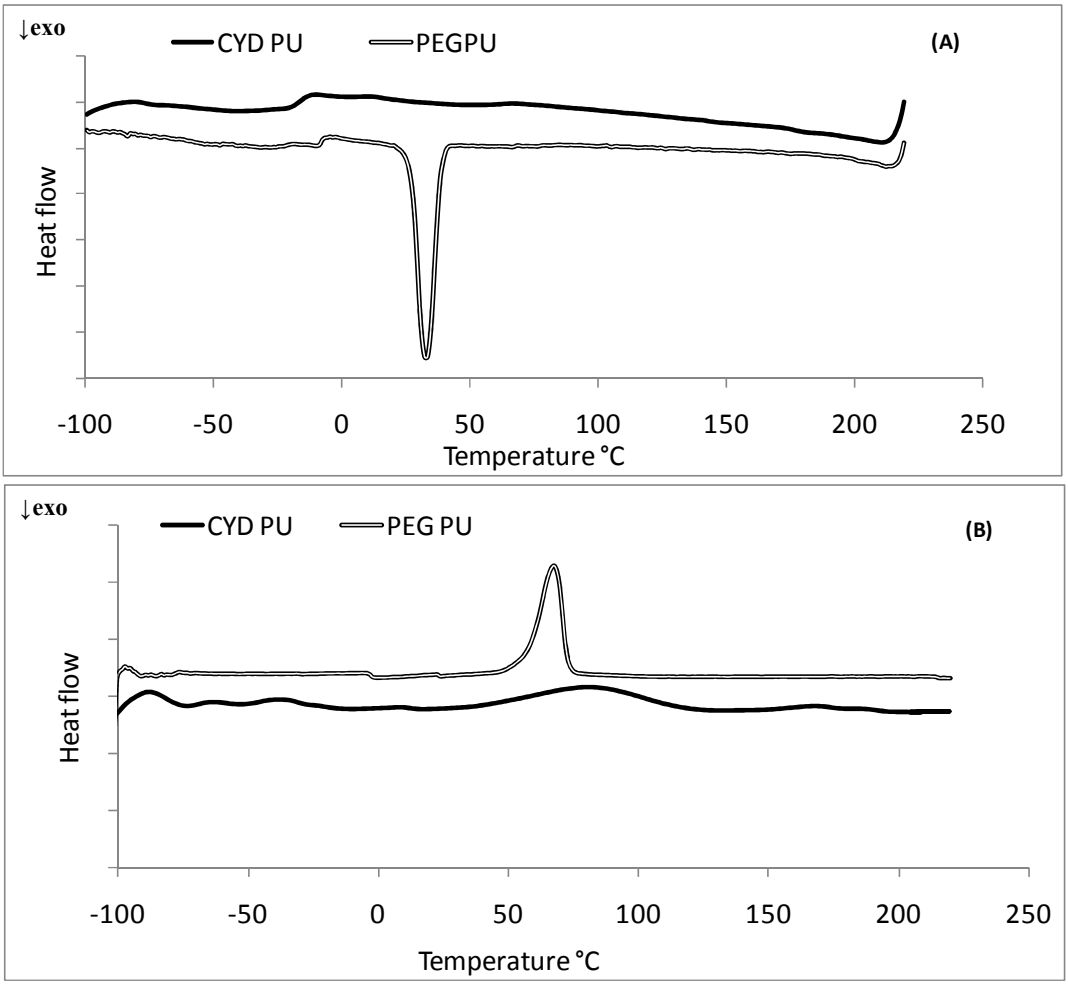

Figure 5.4 (b) DSC thermograms of copolymers

The values of T_{gHS} and T_{gSS} obtained for PEG-PU and CYD-PU is shown in Table 5.2. It can be noted that the values of Tg for PEG-PU is lesser than that for CYD-PU, which can be attributed to highly crosslinked structure of the later. The soft segment involved in PEG-PU is polyethylene glycol with functionality 2, whereas for CYD-PU its β-Cyclodextrin with higher functionality due to presence of multiple hydroxyl groups. The higher functionality of β-Cyclodextrin might be responsible for reaction with higher number of NCO groups of isocyanate leading to high crosslink density.

5.3.4 SEM-EDS ANALYSIS

The morphology of the MNPs is shown in Fig 5.5(a). The pure Fe_3O_4 nanoparticles were observed as small aggregated particles due to their nano size. It was observed that with conjugation of PU on the surface of MNPs, there was increase in size as well as dispersion which might be, as reported by Akbarzadeh et al., due to the electrostatic repulsion force and steric hindrance between the polymer chains on the surface of Fe_3O_4 nanoparticles [46]. Also at magnification of 100X the pure Fe_3O_4 nanoparticles could be observed as agglomerated mass, while PU-MNP nanoconjugates were observed to be discrete particles with higher dimension and without agglomeration. At higher magnification, the particles were observed to be easily distinguishable from one-another and having sharp features in case of pure Fe_3O_4 nanoparticles; but for CYD-PU-11 the image was observed to be blurred and particles were observed to have blunt surface and homogeneity in nature. With increase in isocyanate content for CYD-PU-12, the layered bruises were observed on the surface of nanoparticles that might be assigned to PU [26] conjugated on nanoparticles. The bruises became more apparent for CYD-PU-13 with severely blunt surface suggesting the conjugation of highly crosslinked PU on the surface of nanoparticles.

The EDS spectra showed the elemental fingerprints of nanoparticles (Fig 5.5(b)). The EDS spectra of pure Fe_3O_4 nanoparticles showed strong peaks of Fe and O with weight percent of 71.33% and 27.95% respectively (Table 5.3). However the PU-MNP nanoconjugates showed presence of elemental carbon and higher weight percent of C and O as compare to pure Fe_3O_4 nanoparticles.

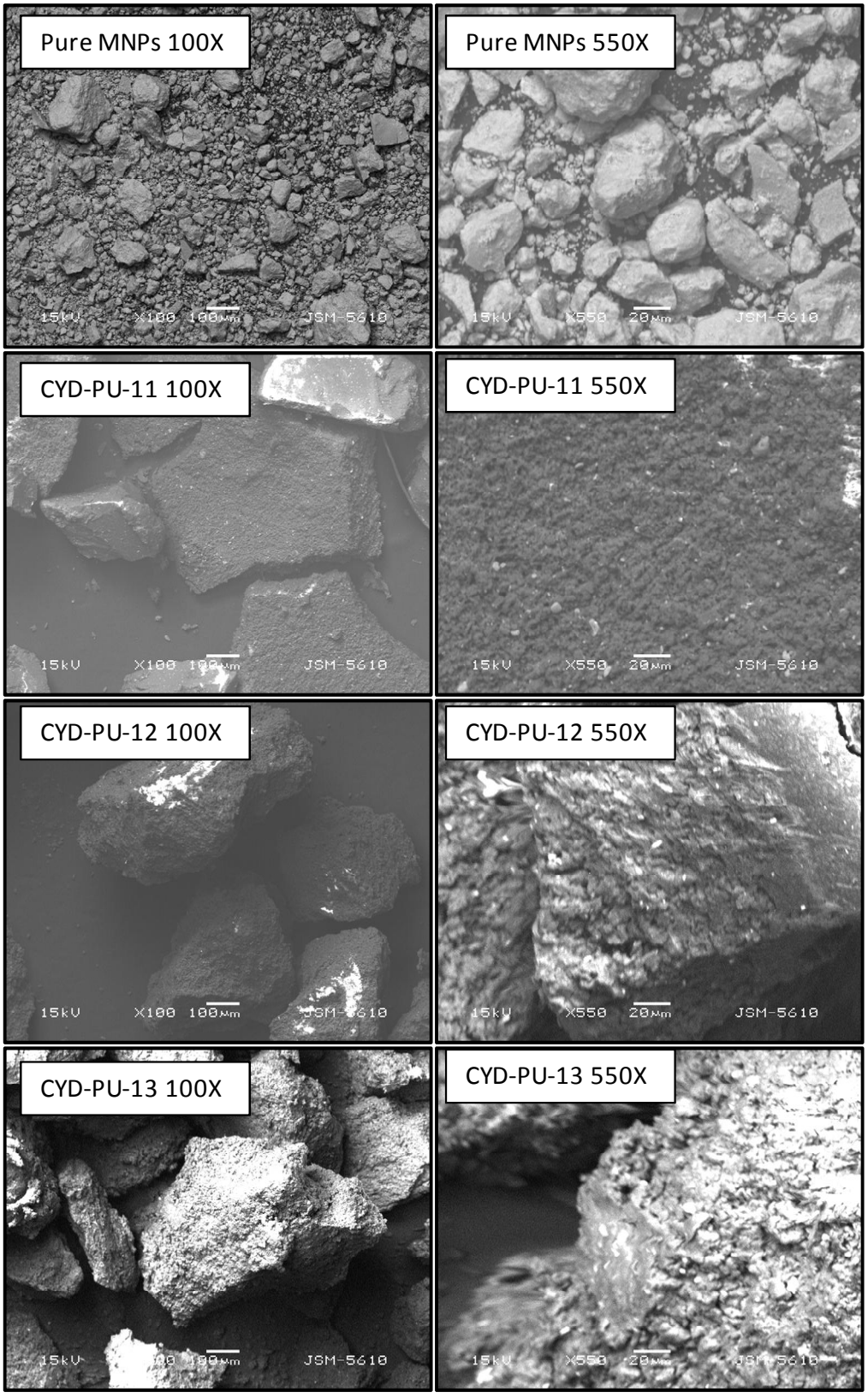

Figure 5.5 (a) SEM micrographs of pure MNPs and PU-MNP nanoconjugates

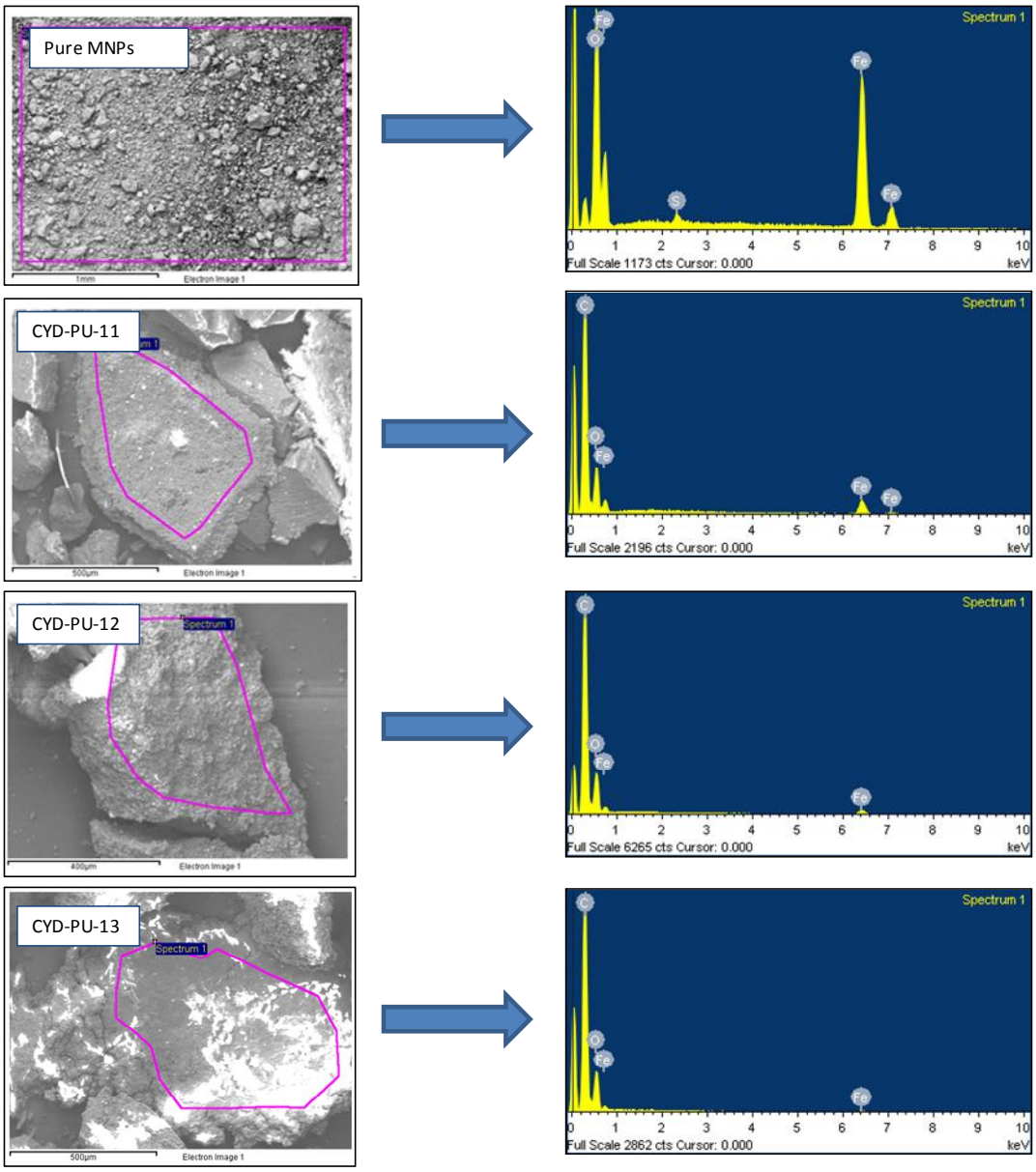

Figure 5.5(b) EDS patterns of pure MNPs and PU-MNP nanoconjugates

This result again confirms the successful conjugation of PU on the surface of Fe_3O_4 nanoparticles. Also, there was increase in the percentage of C and O with increase in the β-Cyclodextrin:HMDI mole ratio, which indicates that with increase in mole ratio, higher content of polymer was conjugated with Fe_3O_4 nanoparticles. This result supports the hypothesis that there was increase in crosslinking of PU with increase in β-Cyclodextrin:HMDI mole ratio.

Table 5.3 Composition of components of pure MNPs and PU MNP nanoconjugates by EDS

Element	Weight%			
	Pure Fe NPs	CYD PU-11	CYD-PU-12	CYD-PU-13
C K	00.00	63.05	66.19	67.48
O K	27.95	25.96	29.45	31.48
Fe K	71.33	10.99	04.36	01.03

5.3.5 TEM ANALYSIS

Fig.5.6 shows the TEM images and size distribution of pure Fe_3O_4 and CYD-PU-13 nanoconjugates. In confirmation with SEM analysis, the pure MNPs were observed to be aggregates of small nanoparticles.

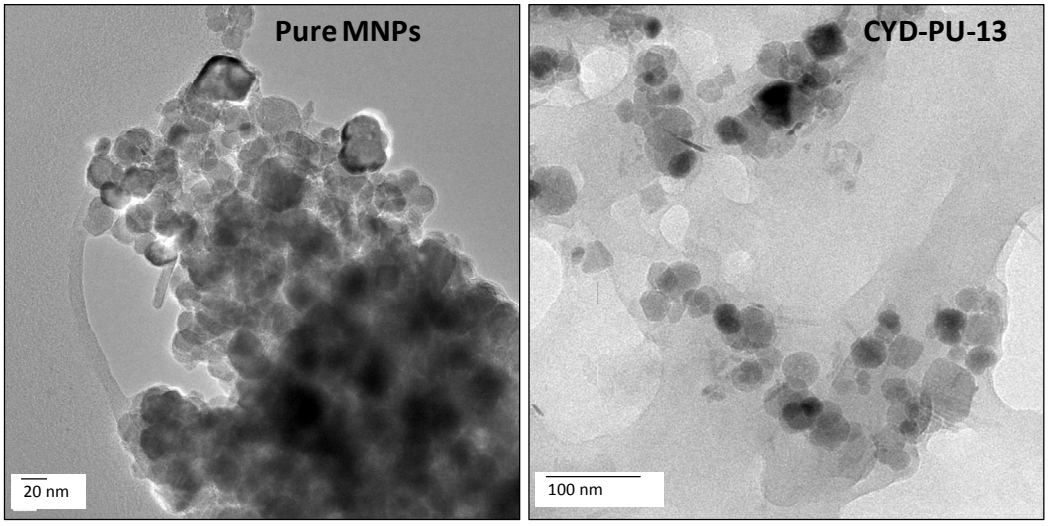

Figure 5.6 TEM images of pure MNPs and PU-MNP nanoconjugates

On the other hand, CYD-PU-13 nanoconjugates were visualized as roughly spherical in shape and more discrete. The nanoconjugates were mono dispersed with narrow size distribution. The difference in dimension of pure MNPs (20-25nm) and PU-MNP nanoconjugates (55-65nm) suggests that the thickness of PU layer might be approximately 35- 40nm. This, once again, suggests successful conjugation of PU on the surface of nanoparticles.

5.3.6 VSM ANALYSIS

The hysteresis loops of magnetic nanoparticles before and after drug loading are shown in Fig. 5.7(a-c). The coercivity, retentivity and magnetic saturation values are depicted in Table 5.4. It is observed that the magnetic saturation value of the CYD-PU-NPs was higher than PEG-PU-NPs, which signifies comparatively higher magnetization of CYD-PU-NPs. As discussed earlier, there is a possibility that PEG may coat the surface of MNPs, which also results in reduction of the magnetic properties of PEG-PU-NPs. Amongst β-Cyclodextrin based nanoconjugates, with increase in β-Cyclodextrin:HMDI mole ratio, the magnetization decreases. This could be attributed to higher load of PU matrix on the magnetic nanoparticles with higher β-Cyclodextrin:HMDI mole ratio. The magnetization value of drug loaded nanoparticles was reduced due to presence of drug molecules on the surface, which also signifies successful loading of drug.

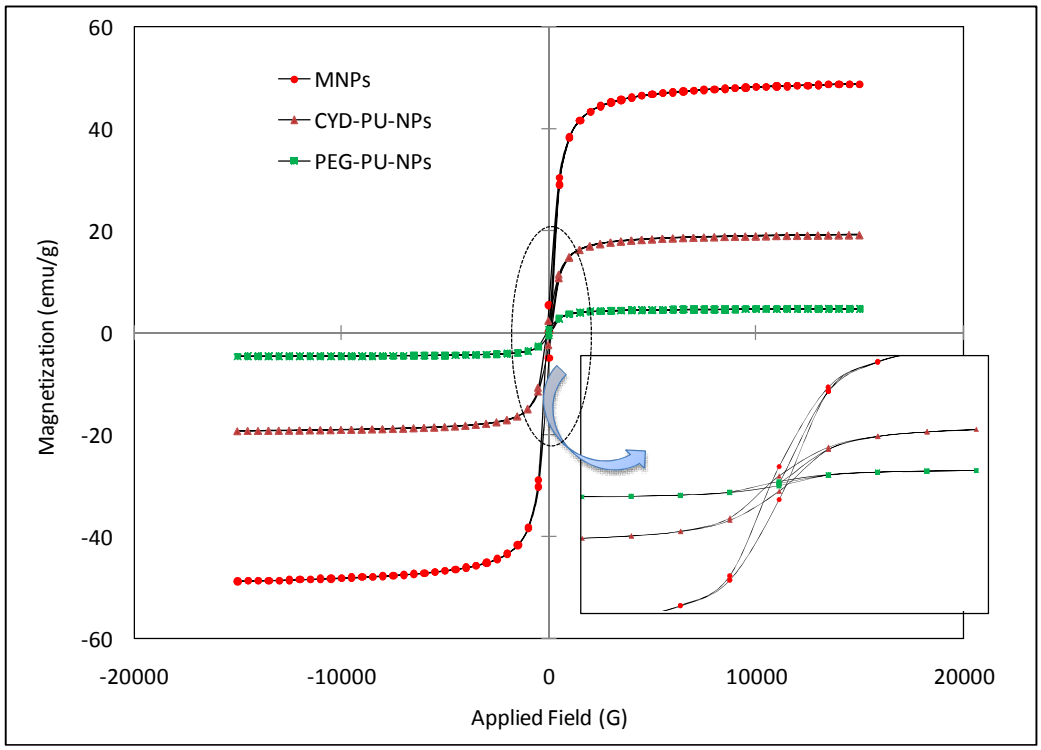

Figure 5.7 (a) Room temperature magnetization curves of pure MNPs and PU-MNP nanoconjugates (before drug loading)

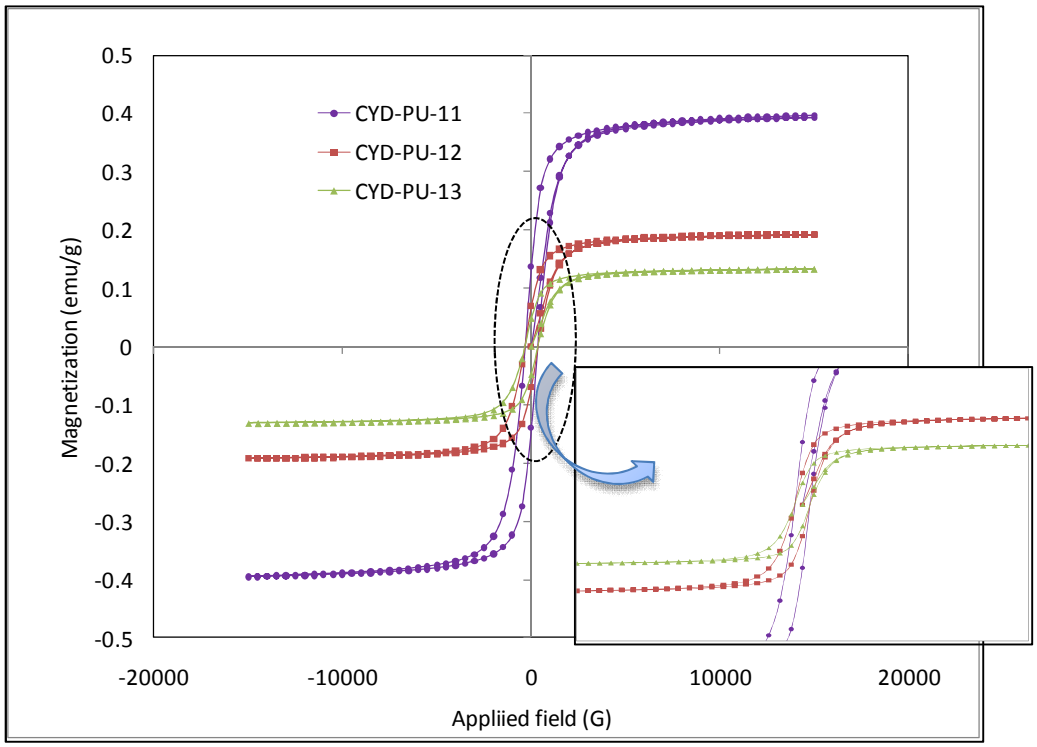

Figure 5.7 (b) Room temperature magnetization curves of CYD-PU-MNPs

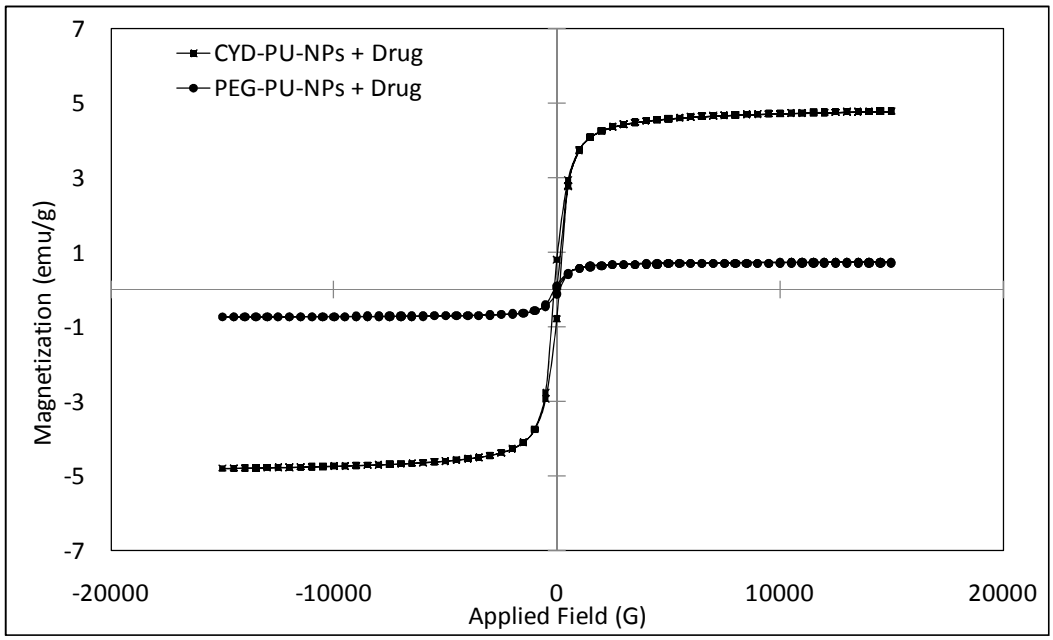

Figure 5.7 (c) Room temperature magnetization curves of nanoconjugates after drug loading

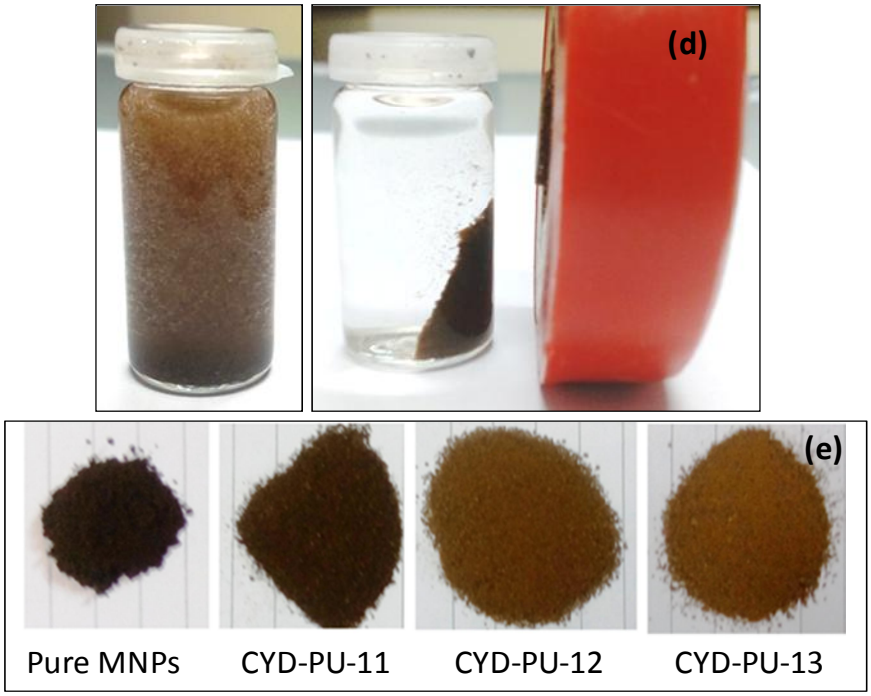

Figure 5.7 (d) Stability and response to magnet for PU-MNP nanoconjugates and **(e)** Visual appearance of pure MNPs and of PU-MNP nanoconjugates

Table 5.4 Retentivity and magnetization values of PU-MNP nanoconjugates

Sample	Magnetization (emu/g)	Coercivity(G)	Retentivity (emu)
Pure Fe_3O_4 MNPs	46.5681	076.12	0.1092
CYD-PU-11	11.0417	336.92	d0.1380
CYD-PU-12	05.0618	346.67	0.0694
CYD-PU-13	03.2932	345.99	0.0476
PEG-PU-NPs	04.6563	098.94	0.0196
drug loaded CYD-PU-12	04.7869	111.49	0.0182
drug loaded PEG-PU-NPs	00.7241	108.07	0.0035

Magnetization curves reveal the ferromagnetic behavior of the PU grafted nanoparticles. All the nanoparticles could be easily dispersed in distilled water and could be drawn from the solution to the wall of the vial by application of external magnet as shown in Fig 5.7(d). Thus, it is clear that even after conjugation with PU the magnetic behavior of the MNPs is retained. As a result, the nanoparticles have excellent magnetic response as desired for intended application in the field drug delivery of anti-cancer drugs. Also, as shown in Fig.5.7 (e), the visual change in color of PU-MNP nanoconjugates can be seen with the change in β-Cyclodextrin:HMDI mole ratio.

5.3.7 XRD ANALYSIS

The XRD patterns of pure Fe_3O_4 nanoparticles and β-Cyclodextrin based PU-MNP nanoconjugates are shown in Fig. 5.8. The XRD pattern of pure Fe_3O_4 nanoparticles exhibited the peaks at 2θ=30.34°, 35.41°, 56.72° and 62.73°, which correspond to (220), (311), (511) and (440) planes of Fe_3O_4, respectively. This could be indexed to its inverse cubic spinal structure [47].

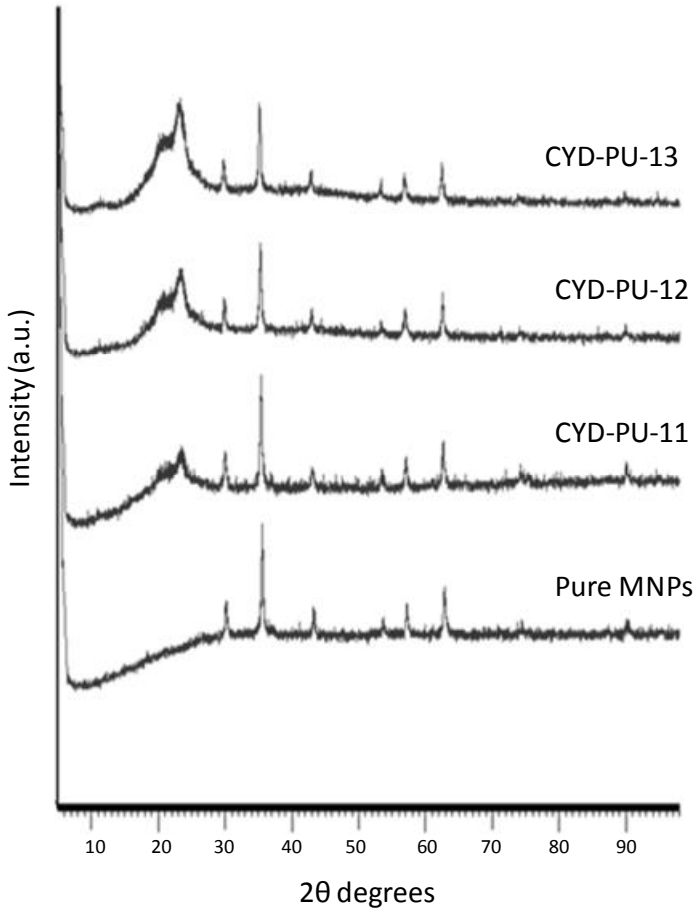

Figure 5.8 XRD patterns of pure Fe_3O_4 MNPs and PU-MNPs nanoconjugates

The presence of all the peaks corresponding to Fe_3O_4 in CYD-PU-NPs reveals that the conjugation of PU on its surface did not lead to change their crystal phase structure [46]. Such types of results have been reported for Fe_3O_4 bonded with hyperbranched

PUs and multiwalled carbon nanotubes [48]. The XRD diffractograms CYD-PU-FeNPs exhibited peaks of Fe_3O_4 along with the peak at 23.65°, 23.48° and 23.53° with relative intensities of 2.98%, 28.37% and 29.46% for CYD-PU-11, CYD-PU-12 and CYD-PU-13 respectively; which corresponds to Cyclodextrin–PU polymer [33]. The increase in the relative intensity of this peak with increase in β-Cyclodextrin:HMDI mole ratio is attributed to the fact that the increased crosslinking of PU resulted into higher hard segment content, resulting in the enhancement of crystallinity of the CYD-PU-FeNPs. The results obtained in XRD analysis thus confirm successful conjugation of PU on Fe_3O_4 nanoparticles along with the changes in their crosslinking behavior with varying β-Cyclodextrin:HMDI mole ratios.

5.3.8 SWELLING STUDIES

The PUs are reported to have direct correlation between swelling and crosslink density. The lesser the crosslinking, the higher is the flexibility and swelling [49]. As shown in Table 5.5, the equilibrium swelling of PEG-PU-NPs was observed to be three fold higher than that of CYD-PU-NPs. This is due to the structural flexibility and reduced crosslinking of PEG-PU- NPs as compared to CYD-PU-NPs, which is again in accordance with thermal analysis.

5.3.9 DRUG LOADING AND RELEASE STUDIES

As shown in Table 5.5, the drug loading capacity of CYD-PU-NPs was greater than PEG-PU-NPs. In the present case, β-Cyclodextrin was expected to offer dual advantages for drug delivery. Firstly, being multihydroxyl compound it can lead to formation of crosslinked urethane network. Secondly, it can form inclusion complex with drug. As a result of both these factors there is an increased drug loading. This kind of behavior is very common for β-Cyclodextrin functionalized polymers as

reported for inclusion of various drugs by hydroxypropyl β-Cyclodextrin [8,22,50–52] Moreover, monovinyl β-Cyclodextrin based nanoparticles showed enhanced regulation for delivery of campthothecin [53].

Table 5.5 Swelling coefficient (Q) for PU-MNP nanoconjugates; entrapment efficiency (%LE) and drug release kinetics' constants for nanoparticles

Sample	%LE	Q	n value	k value
PEG-PU-NPs	05.589	8.0752	0.6418	1.48
CYD-PU-11	14.028	2.6958	0.6305	1.63
CYD-PU-12	11.361	2.4589	0.6165	1.60
CYD-PU-13	08.021	2.2589	0.8419	2.12

The drug release study was carried out in phosphate buffer saline at pH 7.4 at 37°C under dark conditions. All the studies were conducted thrice and the mean values were used to construct plot for drug release studies. Fig. 5.9 shows the release profiles of Dacarbazine-loaded PEG-PU-NPs and CYD-PU-NPs as a function of time. It was observed that PEG-PU-NPs showed higher rate of drug release as compared to CYD-PU-NPs. The drug was released within a shorter period of time with a burst type of release (initial rapid release of 45% of drug release during first 40 min) in case of PEG-PU-NPs. This is attributed to higher swelling coefficient of PEG-PU-NPs as compared to CYD-PU-NPs. The drug release in case of PEG-PU-NPs thus follows diffusion mechanism as observed for other reported PUs [25,26]. However, in case of

CYD-PU-NPs, the drug release behavior was entirely different as it was observed to be slower and sustained. For CYD-PU-NPs, the drug release profile was characterized by an initial rapid release of 5-15% of drug release during first 20-25 min followed by comparatively slower rate of release of remaining drug. This observation suggests that a portion of the drug-Cyclodextrin complex in the nanoparticles is quite labile and the rest portion is apparently stable. In case of CYD-PU-NPs, in addition to diffusion mechanism , the role of Cyclodextrin as a host to form drug-Cyclodextrin complex formation also plays an important role in release of drug. The labile portion is thus hypothesized to be released due to the swelling effect of the PU while later sustained and slower release is attributed to dissociation of drug-Cyclodextrin complex. The hydrophobic part of Dacarbazine interacts with hydrophobic cavity of β-Cyclodextrin [54] which may lead to higher stabilization of drug-Cyclodextrin complex contributing in slowing the release down.

To further study the role of Cyclodextrin in drug release properties, we carried out drug loading and release study for CYD-PU-11, CYD-PU-12 and CYD-PU-13. As shown in Table 5.5, the drug loading capacity of nanoparticles decreased from 14.028% to 8.021% as mole ratio of β-Cyclodextrin:HMDI increased from 1:1 to 1:3. This can be explained based on our hypothesis that size of cavity reduces with increase in β-Cyclodextrin:HMDI mole ratio. The formation of inclusion complex between the drug molecule and Cyclodextrin is simply a dimensional fit between the host cavity and the guest molecule [16,55]. The hydrophobic cavity of Cyclodextrin provides a platform for the suitably sized non-polar drug molecules to be entrapped into the cavity. The mechanism of such host-guest type complex formation involves no formation/breaking of covalent bonds; rather it involves the release of enthalpy-rich water molecules from the cavity. The water molecules thus released get displaced

by more hydrophobic guest molecules which results in apolar-apolar association and decrease of ring strain of Cyclodextrin [56].

The loading of drug in case of CYD-PU-NPs depends on both the crosslink density of PU and size of cavity of β-Cyclodextrin. The increase of crosslink density of PU and decrease of cavity size of β-Cyclodextrin with increase in mole ratio of β-Cyclodextrin:HMDI finally leads to decrease in drug loading capacity of parent nanoparticles. Similarly, the rate of drug release also decreased with increasing mole ratio of β-Cyclodextrin:HMDI. The important observation is that in all the three cases, the initial release of 23-26% of drug was observed to be rapid and similar while later portion of drug showed different release rate. This supports our hypothesis that the swelling property of PU is responsible for initial rate of release. Dissociation of inclusion complex is usually a process driven by large increase in the number of water molecules in the surrounding environment that can again displace the guest molecules from the cavity[41]. During the course of 430 min, the total percentage of cumulative release observed was 54%, 72% and 96% for CYD-PU-11, CYD-PU-12 and CYD-PU-13 respectively. The reduction in release rate is due to enhanced capacity of Cyclodextrin to provide better hosting to encapsulated drug due to smaller cavity size in case of CYD-PU-11. Since diffusion of drug from smaller cavity may be more resistive as compared to bigger cavity [7,57,58], the rate of drug release was compromised.

It is noteworthy that although PEG-PU-NPs showed higher rate of drug release, the pattern of such release rate is not favorable for controlled drug delivery applications. This is because the burst release is unpredictable, and even in the cases where burst release is desired, the amount of burst cannot be significantly controlled. Also there is

danger of high concentration of drug release in short time in the amounts of the drug which can be beyond the toxic level in vivo [59].

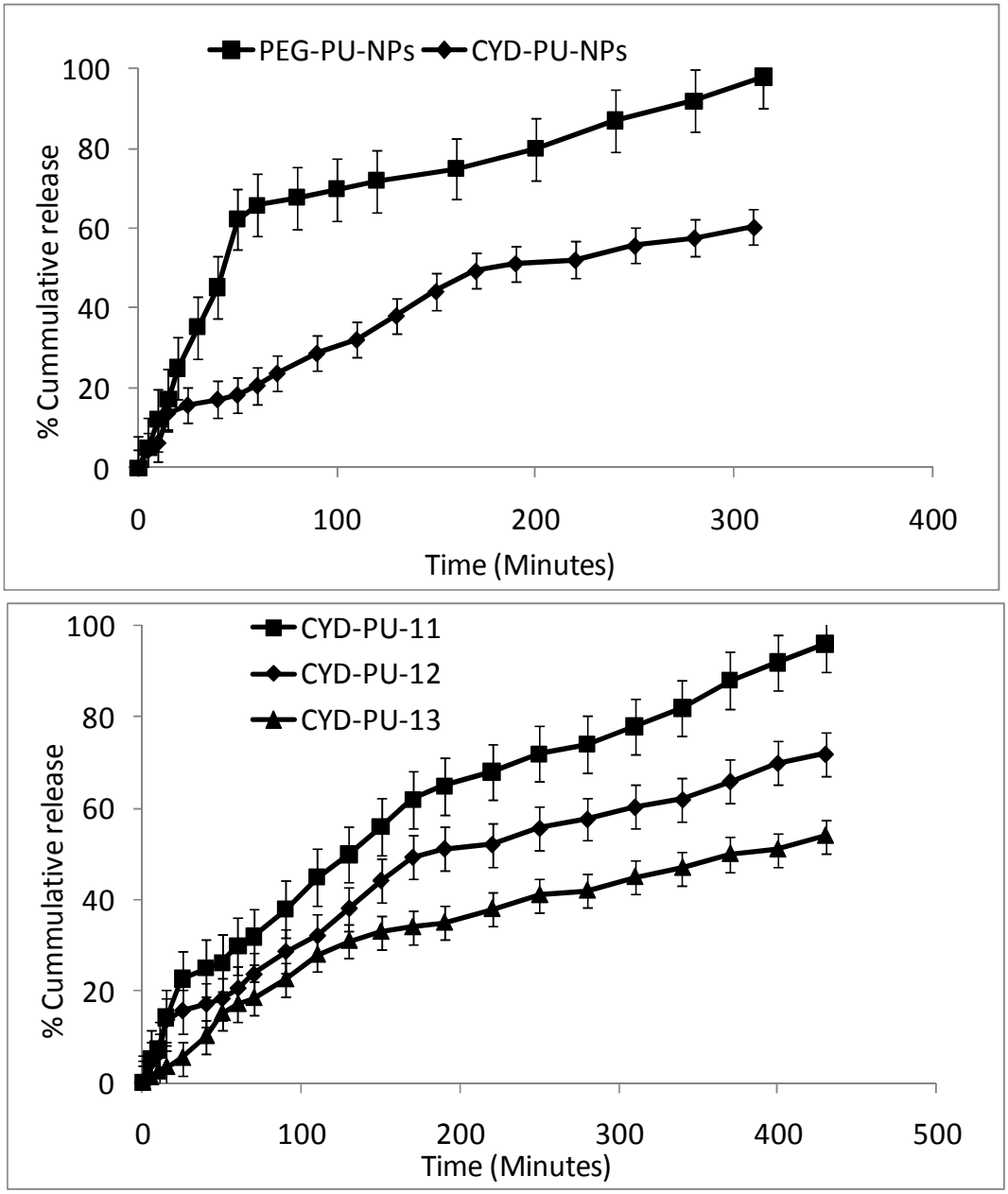

Figure 5.9 Drug release profiles of PU-MNPs nanoconjugates

The drug released during the burst might also get metabolized and excreted without being effectively utilized. Such wastage of drug may incur drug dosage loss and

economic loss [60]. All of these disadvantages could be overcome by utilizing β-Cyclodextrin in the synthesis of PU, which offers well-controlled rate of drug release as described above.

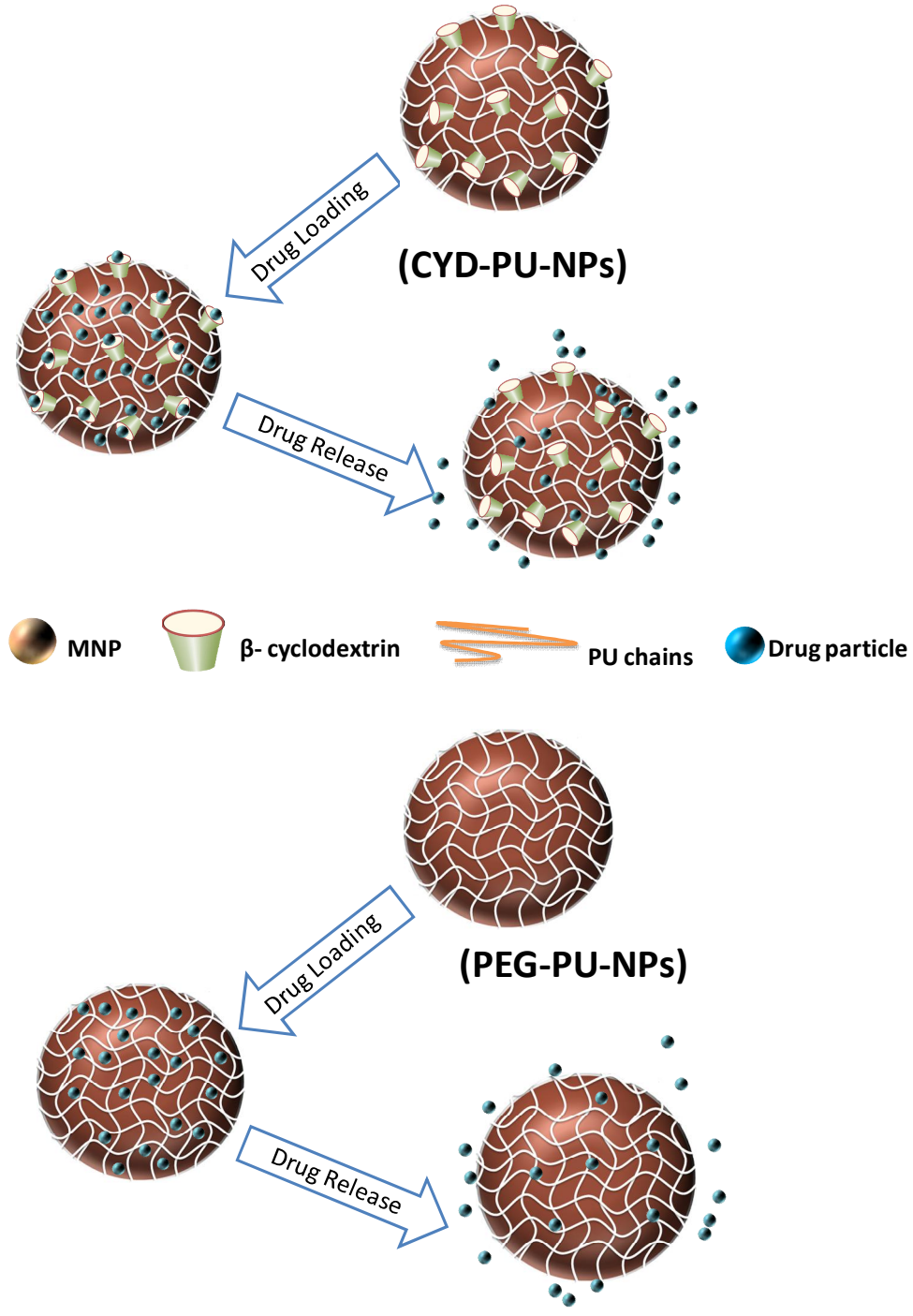

Scheme 2 Schematic of drug loading and release from PU-MNPs nanoconjugates

A schematic diagram of drug loading and release for CYD-PU-MNPs and PEG-PU-MNPs is shown in scheme 2. The additional benefit of combination of PU with β-Cyclodextrin is that by controlling the stoichiometry of PU formation, the number of hydroxyl groups on the Cyclodextrin molecule could be controlled. This could give control over surface accessible inclusion sites, giving command over drug release rate. The kinetics of drug release pattern of MNPs was studied by method reported by Ritger et al [61]. For this purpose following equation was used, where the M_t/ M_∞ denotes a portion of drug released at time t (M_∞ is considered same as the amount total drug loaded in each polymer), k is constant of release rate and n is an important exponent value which can be used to define release mechanism.

$$\frac{M_t}{M_\infty} = kt^n \qquad \text{---------- (3)}$$

The results obtained from the plot shown in Fig. 5.9 were used to outline the graph of log (M_t/M_∞) versus log (t). The intercept and slope obtained using the trend line equation gave the values of k and n respectively. As shown in Table 5.5, the values of n were beyond 0.5, which according to Ritger et al, signifies that the release mechanism involved in the present systems follows non-Fickian diffusion.

5.3.10 MTT Assay

The plot of %cell viability for PEG-PU-NPs and CYD-PU-NPs derived from the MTT assay confirms the non-cytotoxicity of nanoconjugates. It was observed from the representative plot (Fig. 5.10) that even after duration of 24h the MTT absorbance of the media exposed to nanoconjugates was very near to control and well below toxicity limit. This result confirms that there was no leaching of harmful toxins from nanoparticles. Hence, the prepared set of nanoconjugates can find application in the field of biocompatible drug carriers.

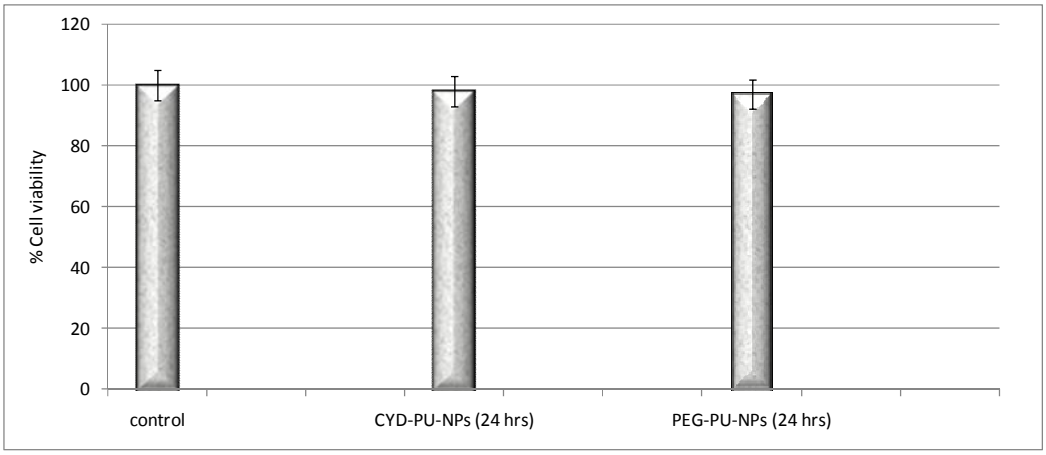

Figure 5.10 Cell viability of PEG-PU-NPs and CYD-PU-NPs by MTT assay

5.4. CONCLUSIONS

Fe_3O_4 nanoparticles were conjugated with β-Cyclodextrin/PEG by urethane linkage to prepare PU-MNP nanoconjugates namely CYD-PU-NPs/PEG-PU-NPs. The nanoconjugates were characterized by FTIR, XRD, SEM-EDS and VSM analysis. The thermal analysis showed that PEG-PU-NPs were observed to possess higher thermal stability, less magnetization and burst release profile, whereas CYD-PU-NPs showed reasonable thermal stability, magnetization and controlled drug release profile.

Dacarbazine, an anticancer drug was considered as a model drug for loading and release studies. By controlling the mole ratio of β-Cyclodextrin to HMDI, it was feasible to get command over cavity size of β-Cyclodextrin. This aided in achieving the control over entrapment efficiency and release behavior of MNPs, which ultimately served the purpose of controlled drug release. The Dacarbazine-loaded nanoparticles are found to be non-toxic and could form stable water dispersions, which presumably are expected to reduce the serious side effects encountered by chemotherapy. The approach of utilizing synergistic advantage of PU, Cyclodextrin

and magnetic nano particles invites attractive application of prepared nano carriers in the field of cancer therapy. The prepared nanocarriers thus can provide a strong platform for magnetic tumor targeting under guidance of magnetic field and through cyclodextin-drug complexation.

5.5 REFERENCES

[1] J. Dobson, J.D. Ã, Magnetic nanoparticles for drug delivery, Drug Dev. Res. 67 (2006) 55–60. doi:Doi 10.1002/Ddr.20067.

[2] B. Chertok, A.E. David, V.C. Yang, Brain tumor targeting of magnetic nanoparticles for potential drug delivery: effect of administration route and magnetic field topography, J Control Release. 155 (2011) 393–399. doi:10.1016/j.jconrel.2011.06.033.

[3] T. Neuberger, B. Schopf, H. Hofmann, M. Hofmann, B. Vonrechenberg, Superparamagnetic nanoparticles for biomedical applications: Possibilities and limitations of a new drug delivery system, J. Magn. Magn. Mater. 293 (2005) 483–496. doi:10.1016/j.jmmm.2005.01.064.

[4] A.J. Cole, A.E. David, J. Wang, C.J. Galbán, H.L. Hill, V.C. Yang, Polyethylene glycol modified, cross-linked starch-coated iron oxide nanoparticles for enhanced magnetic tumor targeting., Biomaterials. 32 (2011) 2183–93. doi:10.1016/j.biomaterials.2010.11.040.

[5] Y. Liu, K. Yang, L. Cheng, J. Zhu, X. Ma, H. Xu, et al., PEGylated FePt@Fe2O3 core-shell magnetic nanoparticles: potential theranostic applications and in vivo toxicity studies., Nanomedicine. 9 (2013) 1077–88. doi:10.1016/j.nano.2013.02.010.

[6] A.P. Plazzo, C.T. Höfer, L. Jicsinszky, É. Fenyvesi, L. Szente, J. Schiller, et al., Uptake of a fluorescent methyl-β-cyclodextrin via clathrin-dependent endocytosis., Chem. Phys. Lipids. 165 (2012) 505–11. doi:10.1016/j.chemphyslip.2012.03.007.

[7] J.L. Beckett, C.J. Hartzell, N.L. Eastman, T. Blake, M.P. Eastman, Cyclodextrin Complexation of the Tetracyanoquinodimethane Anion Radical - the Chemical Consequences of Cavity Size and Alkyl Derivatization, J. Org. Chem. 57 (1992) 4173–4179. doi:Doi 10.1021/Jo00041a022.

[8] S. Sajeesh, C.P. Sharma, Cyclodextrin-insulin complex encapsulated polymethacrylic acid based nanoparticles for oral insulin delivery., Int. J. Pharm. 325 (2006) 147–54. doi:10.1016/j.ijpharm.2006.06.019.

[9] R. Yang, J.B. Chen, X.Y. Dai, R. Huang, C.F. Xiao, Z.Y. Gao, et al., Inclusion complex of GA-13315 with cyclodextrins: Preparation, characterization, inclusion mode and properties, Carbohydr. Polym. 89 (2012) 89–97. doi:10.1016/j.carbpol.2012.02.054.

[10] I. Miyazawa, H. Ueda, H. Nagase, T. Endo, S. Kobayashi, T. Nagai, Physicochemical properties and inclusion complex formation of δ-cyclodextrin, Eur. J. Pharm. Sci. 3 (1995) 153–162. doi:10.1016/0928-0987(95)00006-Y.

[11] M.R. de Freitas, L.A. Rolim, M.F.D.L.R. Soares, P.J. Rolim-Neto, M.M. de Albuquerque, J.L. Soares-Sobrinho, Inclusion complex of methyl-β-cyclodextrin and olanzapine as potential drug delivery system for schizophrenia., Carbohydr. Polym. 89 (2012) 1095–100. doi:10.1016/j.carbpol.2012.03.072.

[12] T.A. Nguyen, B. Liu, J. Zhao, D.S. Thomas, J.M. Hook, An investigation into the supramolecular structure, solubility, stability and antioxidant activity of rutin/cyclodextrin inclusion complex, Food Chem. 136 (2013) 186–192. doi:10.1016/j.foodchem.2012.07.104.

[13] S. Sundar, R. Mariappan, S. Piraman, Synthesis and characterization of amine

modified magnetite nanoparticles as carriers of curcumin-anticancer drug, Powder Technol. 266 (2014) 321–328. doi:10.1016/j.powtec.2014.06.033.

[14] A.Z.M. Badruddoza, M.T. Rahman, S. Ghosh, M.Z. Hossain, J. Shi, K. Hidajat, et al., β-Cyclodextrin conjugated magnetic, fluorescent silica core-shell nanoparticles for biomedical applications, Carbohydr. Polym. 95 (2013) 449–457. doi:10.1016/j.carbpol.2013.02.046.

[15] M.H. Mohamed, L.D. Wilson, J. V. Headley, Estimation of the surface accessible inclusion sites of β-cyclodextrin based copolymer materials, Carbohydr. Polym. 80 (2010) 186–196. doi:10.1016/j.carbpol.2009.11.014.

[16] K. Uekama, F. Hirayama, T. Irie, Cyclodextrin Drug Carrier Systems, Chem Rev. 98 (1998) 2045–2076 ST – Cyclodextrin Drug Carrier Systems. doi:10.1021/cr970025p.

[17] A.R. Khan, P. Forgo, K.J. Stine, V.T. D'Souza, Methods for Selective Modifications of Cyclodextrins., Chem. Rev. 98 (1998) 1977–1996. doi:10.1021/cr970012b.

[18] F. Van De Manakker, T. Vermonden, C.F. Van Nostrum, W.E. Hennink, Cyclodextrin-based polymeric materials: Synthesis, properties, and pharmaceutical/biomedical applications, Biomacromolecules. 10 (2009) 3157–3175. doi:10.1021/bm901065f.

[19] K.Y. Win, S.-S. Feng, Effects of particle size and surface coating on cellular uptake of polymeric nanoparticles for oral delivery of anticancer drugs., Biomaterials. 26 (2005) 2713–2722. doi:10.1016/j.biomaterials.2004.07.050.

[20] B. Gidwani, A. Vyas, Synthesis, characterization and application of Epichlorohydrin-β-cyclodextrin polymer, Colloids Surfaces B Biointerfaces.

114 (2014) 130–137. doi:10.1016/j.colsurfb.2013.09.035.

[21] W. Zhang, M. Chen, G. Diao, Preparation and electrochemical behavior of water-soluble inclusion complex of ferrocene with β-cyclodextrin polymer, Electrochim. Acta. 56 (2011) 5129–5136. doi:10.1016/j.electacta.2011.03.062.

[22] E.E.M. Eid, A.B. Abdul, F.E.O. Suliman, M. a. Sukari, a. Rasedee, S.S. Fatah, Characterization of the inclusion complex of zerumbone with hydroxypropyl-β-cyclodextrin, Carbohydr. Polym. 83 (2011) 1707–1714. doi:10.1016/j.carbpol.2010.10.033.

[23] E.P. Akçakoca Kumbasar, Ç. Akduman, A. Çay, Effects of β-cyclodextrin on selected properties of electrospun thermoplastic polyurethane nanofibres, Carbohydr. Polym. 104 (2014) 42–49. doi:10.1016/j.carbpol.2013.12.065.

[24] J.L. Soares-Sobrinho, F.L. a Santos, M. a M. Lyra, L.D.S. Alves, L. a. Rolim, A. a N. Lima, et al., Benznidazole drug delivery by binary and multicomponent inclusion complexes using cyclodextrins and polymers, Carbohydr. Polym. 89 (2012) 323–330. doi:10.1016/j.carbpol.2012.02.042.

[25] A. Solanki, J. Mehta, S. Thakore, Structure-property relationships and biocompatibility of carbohydrate crosslinked polyurethanes., Carbohydr. Polym. 110 (2014) 338–44. doi:10.1016/j.carbpol.2014.04.021.

[26] A.R. Solanki, B. V Kamath, S. Thakore, Carbohydrate crosslinked biocompatible polyurethanes : Synthesis , characterization , and drug delivery studies, 42223 (2015) 1–12. doi:10.1002/app.42223.

[27] F. Zia, K.M. Zia, M. Zuber, S. Kamal, N. Aslam, Starch based polyurethanes: A critical review updating recent literature, Carbohydr. Polym. 134 (2015) 784–798. doi:10.1016/j.carbpol.2015.08.034.

[28] S. Dandamudi, R.B.C. Ã, The drug loading , cytotoxicty and tumor vascular targeting characteristics of magnetite in magnetic drug targeting, 28 (2007) 4673–4683. doi:10.1016/j.biomaterials.2007.07.024.

[29] I. Ahmad, M. Ahmad, International Journal of Biological Macromolecules Dacarbazine as a minor groove binder of DNA : Spectroscopic , biophysical and molecular docking studies, Int. J. Biol. Macromol. 79 (2015) 193–200. doi:10.1016/j.ijbiomac.2015.04.055.

[30] D.C. Lev, A. Onn, V.O. Melinkova, C. Miller, V. Stone, M. Ruiz, et al., Exposure of melanoma cells to dacarbazine results in enhanced tumor growth and metastasis in vivo, J. Clin. Oncol. 22 (2004) 2092–2100. doi:10.1200/JCO.2004.11.070.

[31] V.P. Torchilin, Targeted polymeric micelles for delivery of poorly soluble drugs, Cell. Mol. Life Sci. 61 (2004) 2549–2559. doi:10.1007/s00018-004-4153-5.

[32] S. Kakumanu, J.B. Tagne, T.A. Wilson, R.J. Nicolosi, A nanoemulsion formulation of dacarbazine reduces tumor size in a xenograft mouse epidermoid carcinoma model compared to dacarbazine suspension, Nanomedicine Nanotechnology, Biol. Med. 7 (2011) 277–283. doi:10.1016/j.nano.2010.12.002.

[33] A.R. Kiasat, S. Nazari, Magnetic nanoparticles grafted with β-cyclodextrin–polyurethane polymer as a novel nanomagnetic polymer brush catalyst for nucleophilic substitution reactions of benzyl halides in water, J. Mol. Catal. A Chem. 365 (2012) 80–86. doi:10.1016/j.molcata.2012.08.012.

[34] A.Z.M. Badruddoza, M.T. Rahman, S. Ghosh, M.Z. Hossain, J. Shi, K.

Hidajat, et al., β-Cyclodextrin conjugated magnetic, fluorescent silica core-shell nanoparticles for biomedical applications., Carbohydr. Polym. 95 (2013) 449–57. doi:10.1016/j.carbpol.2013.02.046.

[35] P. Pradhan, J. Giri, F. Rieken, C. Koch, O. Mykhaylyk, M. Döblinger, et al., Targeted temperature sensitive magnetic liposomes for thermo-chemotherapy, J. Control. Release. 142 (2010) 108–121. doi:10.1016/j.jconrel.2009.10.002.

[36] B. V. Shetty, R.L. Schowen, M. Slavik, C.M. Riley, Degradation of dacarbazine in aqueous solution, J. Pharm. Biomed. Anal. 10 (1992) 675–683. doi:10.1016/0731-7085(92)80096-6.

[37] S. Shah, A. Pal, T. Rajyaguru, R.S.R. Murthy, S. Devi, Lamotrigine-Loaded Polyacrylate Nanoparticles Synthesized Through Emulsion Polymerization, (2007). doi:10.1002/app.

[38] M. Zanetta, N. Quirici, F. Demarosi, M.C. Tanzi, L. Rimondini, S. Farè, Ability of polyurethane foams to support cell proliferation and the differentiation of MSCs into osteoblasts., Acta Biomater. 5 (2009) 1126–36. doi:10.1016/j.actbio.2008.12.003.

[39] K. Can, M. Ozmen, M. Ersoz, Immobilization of albumin on aminosilane modified superparamagnetic magnetite nanoparticles and its characterization, Colloids Surfaces B Biointerfaces. 71 (2009) 154–159. doi:10.1016/j.colsurfb.2009.01.021.

[40] R. Nikolaevichyastrebinsky, V.I. Pavlenko, B. Shukhov, S. Technological, Modifying the Surface of Iron-Oxide Minerals with Organic and Inorganic Modifiers, Middle-East J. Sci. Res. 18 (2013) 1455–1462. doi:10.5829/idosi.mejsr.2013.18.10.7098.

[41] E.M.M. Del Valle, Cyclodextrins and their uses: A review, Process Biochem. 39 (2004) 1033–1046. doi:10.1016/S0032-9592(03)00258-9.

[42] A. Solanki, S. Thakore, Cellulose crosslinked pH-responsive polyurethanes for drug delivery: α-hydroxy acids as drug release modifiers, Int. J. Biol. Macromol. 80 (2015) 683–691. doi:10.1016/j.ijbiomac.2015.07.003.

[43] L. Rueda, a Saralegui, B. Fernández d'Arlas, Q. Zhou, L. a Berglund, M. a Corcuera, et al., Cellulose nanocrystals/polyurethane nanocomposites. Study from the viewpoint of microphase separated structure., Carbohydr. Polym. 92 (2013) 751–7. doi:10.1016/j.carbpol.2012.09.093.

[44] T. Tawa, S. Ito, The Role of Hard Segments of Aqueous Polyurethane-urea Dispersion in Determining the Colloidal Characteristics and Physical Properties, Polym. J. 38 (2006) 686–693. doi:10.1295/polymj.PJ2005193.

[45] L. Rueda-Larraz, B.F. d'Arlas, A. Tercjak, A. Ribes, I. Mondragon, A. Eceiza, Synthesis and microstructure–mechanical property relationships of segmented polyurethanes based on a PCL–PTHF–PCL block copolymer as soft segment, Eur. Polym. J. 45 (2009) 2096–2109. doi:10.1016/j.eurpolymj.2009.03.013.

[46] A. Akbarzadeh, M. Samiei, S.W. Joo, M. Anzaby, Y. Hanifehpour, H.T. Nasrabadi, et al., Synthesis, characterization and in vitro studies of doxorubicin-loaded magnetic nanoparticles grafted to smart copolymers on A549 lung cancer cell line., J. Nanobiotechnology. 10 (2012) 46. doi:10.1186/1477-3155-10-46.

[47] J.O. Park, K.Y. Rhee, S.J. Park, Silane treatment of Fe3O4 and its effect on the magnetic and wear properties of Fe3O4/epoxy nanocomposites, Appl. Surf. Sci. 256 (2010) 6945–6950. doi:10.1016/j.apsusc.2010.04.110.

[48] H. Kalita, N. Karak, Bio-Based Hyperbranched Polyurethane / Multi-Walled Carbon Nanotube Nanocomposites as Shape Memory Materials, J. Nanoeng. Nanomanufacturing. 3 (2013) 194–201. doi:10.1002/pc.

[49] F.M. Pardini, J.I. Amalvy, Synthesis and swelling behavior of pH-responsive polyurethane/poly[2-(diethylamino)ethyl methacrylate] hybrid materials, J. Appl. Polym. Sci. 131 (2014) n/a–n/a. doi:10.1002/app.39799.

[50] K.R. Parmar, K.A. Patel, S.R. Shah, N.R. Sheth, Inclusion complexes of lamotrigine and hydroxy propyl β-cyclodextrin: Solid state characterization and dissolution studies, J. Incl. Phenom. Macrocycl. Chem. 65 (2009) 263–268. doi:10.1007/s10847-009-9577-y.

[51] C. Garnero, V. Aiassa, M. Longhi, Sulfamethoxazole:hydroxypropyl-β-cyclodextrin complex: preparation and characterization, J. Pharm. Biomed. Anal. 63 (2012) 74–79. doi:10.1016/j.jpba.2012.01.011.

[52] S. Baboota, S.P. Agarwal, Preparation and characterisation of meloxicam hydroxy propyl beta-cyclodextrin inclusion complex, J. Incl. Phenom. Macrocycl. Chem. 51 (2005) 219–224.

[53] Y.-Y. Liu, Y. Yu, G.-B. Zhang, M.-F. Tang, Preparation, characterization, and controlled release of novel nanoparticles based on MMA/beta-CD copolymers., Macromol. Biosci. 7 (2007) 1250–1257. doi:10.1002/mabi.200700101.

[54] R. Baktiar, Letter: Complexes of amino (6-monodeoxy-6-mono)-β-cyclodextrin probed by electrospray ionization mass spectrometry, Eur. J. Mass Spectrom. 5 (1999) 1. doi:10.1255/ejms.242.

[55] J.B.-M. F.J. Otero-Espinar, J.J. Torres-Labandeira, C. Alvarez-Lorenzo, Cyclodextrins in drug delivery systems, J. Drug Deliv. Sci. Technol. 20 (2010)

289–301.

[56] T. Loftsson, M.E. Brewster, Pharmaceutical applications of cyclodextrins. 1. Drug solubilization and stabilization, J. Pharm. Sci. 85 (1996) 1017–1025. doi:10.1021/js950534b.

[57] Y. Ikeda, F. Hirayama, H. Arima, K. Uekama, Y. Yoshitake, K. Harano, NMR spectroscopic characterization of Metoprolol/cyclodextrin complexes in aqueous solution: Cavity size dependency, J. Pharm. Sci. 93 (2004) 1659–1671. doi:10.1002/jps.20077.

[58] W.C. Cromwell, K. Bystrom, M.R. Eftink, Cyclodextrin-adamantanecarboxylate inclusion complexes: studies of the variation in cavity size, J. Phys. Chem. 89 (1985) 326–332. doi:10.1021/j100248a029.

[59] M.L. Shively, B.A. Coonts, W.D. Renner, J.L. Southard, A.T. Bennett, Physico-chemical characterization of a polymeric injectable implant delivery system, J. Control. Release. 33 (1995) 237–243. doi:10.1016/0168-3659(94)00097-E.

[60] X. Huang, C.S. Brazel, On the importance and mechanisms of burst release in matrix-controlled drug delivery systems, 73 (2001) 121–136.

[61] P.L. Ritger, N.A. Peppas, A simple equation for description of solute release II. Fickian and anomalous release from swellable devices, J. Control. Release. 5 (1987) 37–42. doi:10.1016/0168-3659(87)90035-6.